Supplemental Materials: A Fast Surrogate Model for 3D-Earth Glacial Isostatic Adjustment using Tensorflow (v2.8.10) Artificial Neural Networks

Ryan Love[1], Glenn A. Milne[1], Parviz Ajourlou[1], Soran Parang[1], Lev Tarasov[2], and Konstantin Latychev[3]

[1]Department of Earth Sciences, University of Ottawa, Ottawa, Ontario, Canada
[2]Department of Physics and Physical Oceanography, Memorial University of Newfoundland, St. John's, Newfoundland, Canada
[3]SEAKON, Toronto, Canada

Correspondence: Ryan Love (rlove@mun.ca)

S1 Supplemental Figures

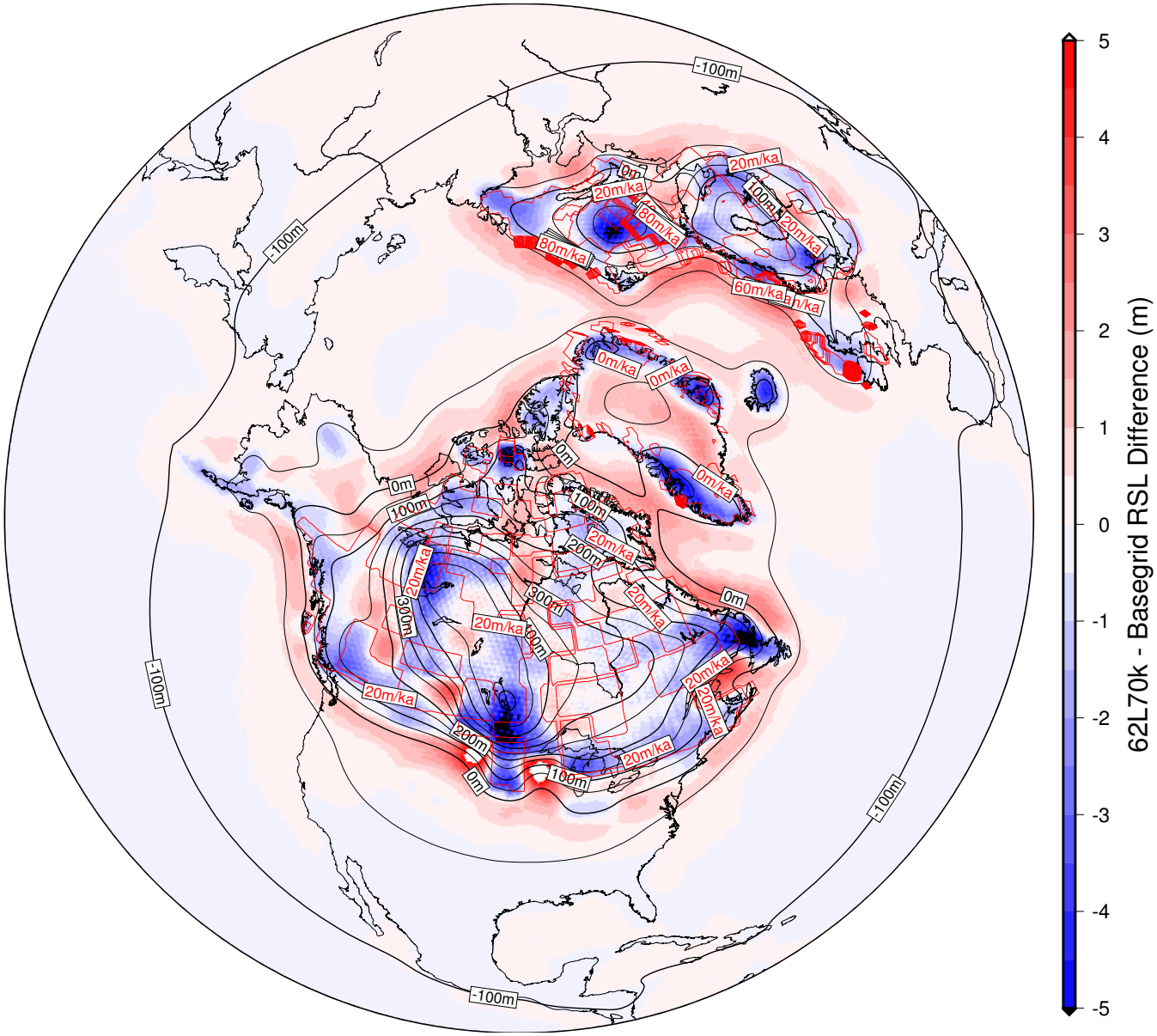

Figure S1. Difference in predicted RSL at LGM between a reduced resolution configuration (62L70k) and the more typical Seakon resolution (Basegrid). Black contours denote the RSL field from the Basegrid configuration at 50 m intervals. The average rate of change in ice thickness between 21 ka and 25 ka, expressed in m/ka, are contoured in red at 10 m/ka intervals. These results are for the ICE5G (Peltier, 2004) ice loading history and background radial viscosity profile of a 120 km thick elastic lithosphere, 3×10^{21} Pa · s upper mantle viscosity, and 90×10^{21} Pa · s lower mantle viscosity. This SS profile was chosen as it performed well for the USEC database in previous investigations (Love et al., 2016). The Seakon model results shown here are comparisons between spherically symmetric configurations. Tests involving lateral variability structure give comparable results.

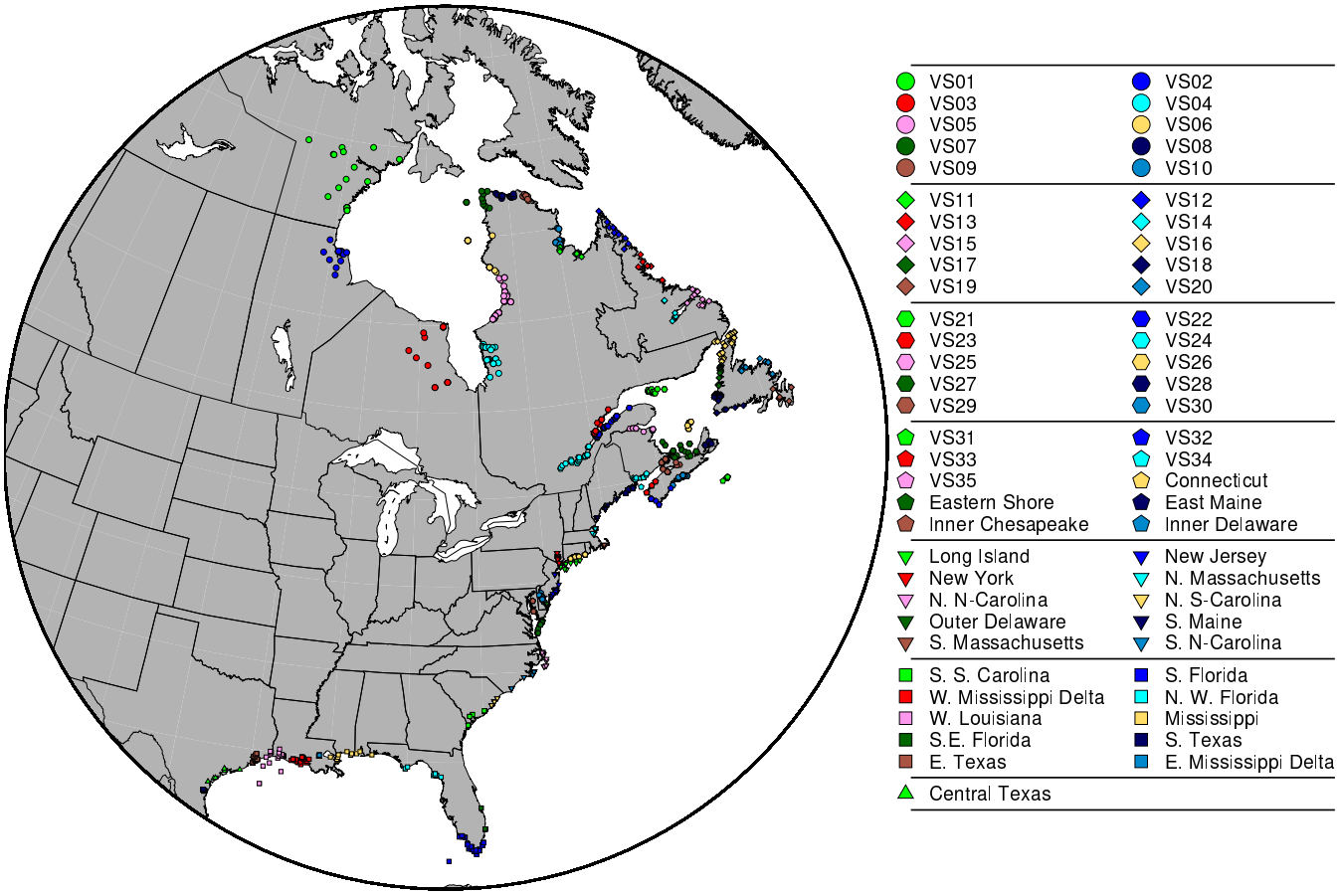

Figure S2. Locations of sea-level index points, terrestrial limiting, marine limiting data are shown as coloured symbols. The shape and colour reflect the groupings of each data-point. VS01 through VS35 are sites 1 through 35 from Vacchi et al. (2018). Connecticut through to S. South-Carolina are from Engelhart and Horton (2012). S.E. Florida to S. Texas are from Love et al. (2016).

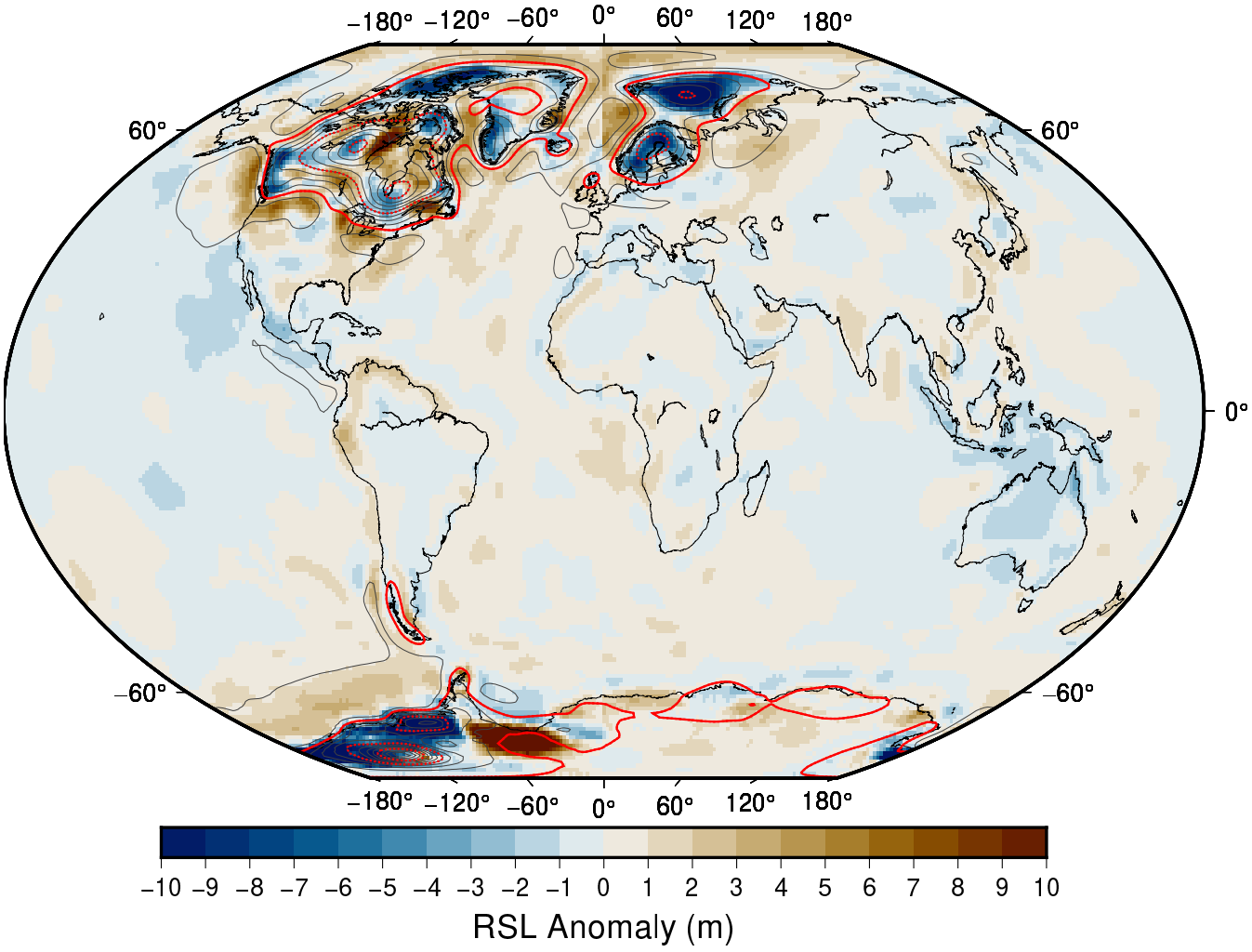

Figure S3. RSL anomaly, emulated RSL field minus explicit (3D-SS Seakon + NMSS) RSL field for the S40RTS+LR18 case, at 10 ka Grey contours denote the RSL field (from Seakon) in 25 m increments, dotted red contours denote 100 m increments, and the solid red contour denotes the 0 m contour. The parameter vector plotted is that with the median MSE, calculated for all spatio-temporal data, for the $N = 45$ results.

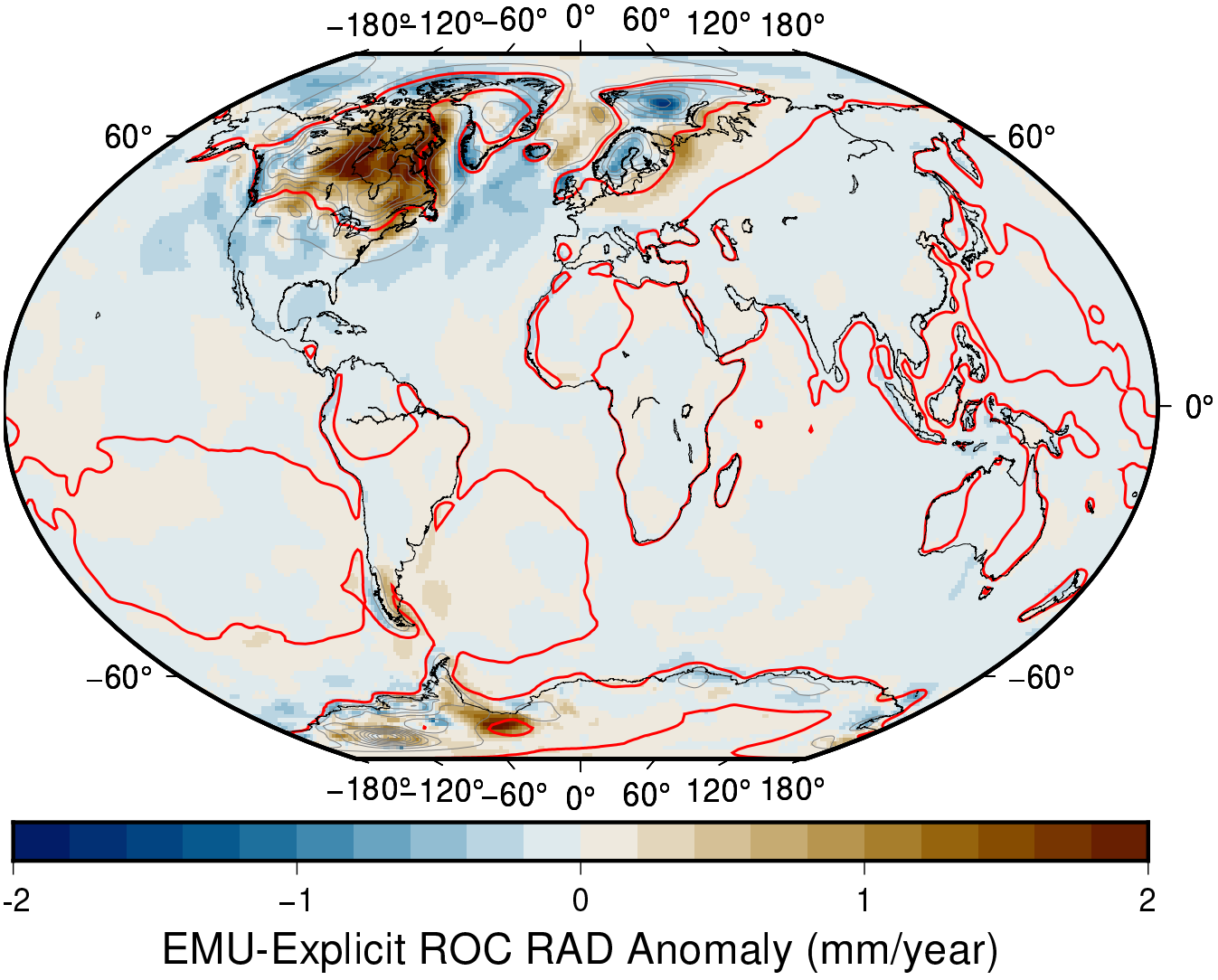

Figure S4. ROC RAD anomaly, emulated field minus 3D-SS field added to the NMSS output for the S40RTS+LR18 case, at present day. Contours denote the ROC RAD field (from from 3D-SS+NMSS) in 2 mm/yr increments, the red line denotes the 0 mm/yr contour. The parameter vector plotted is that with the median MSE, calculated for all spatio-temporal data, for the $N = 45$ ANN.

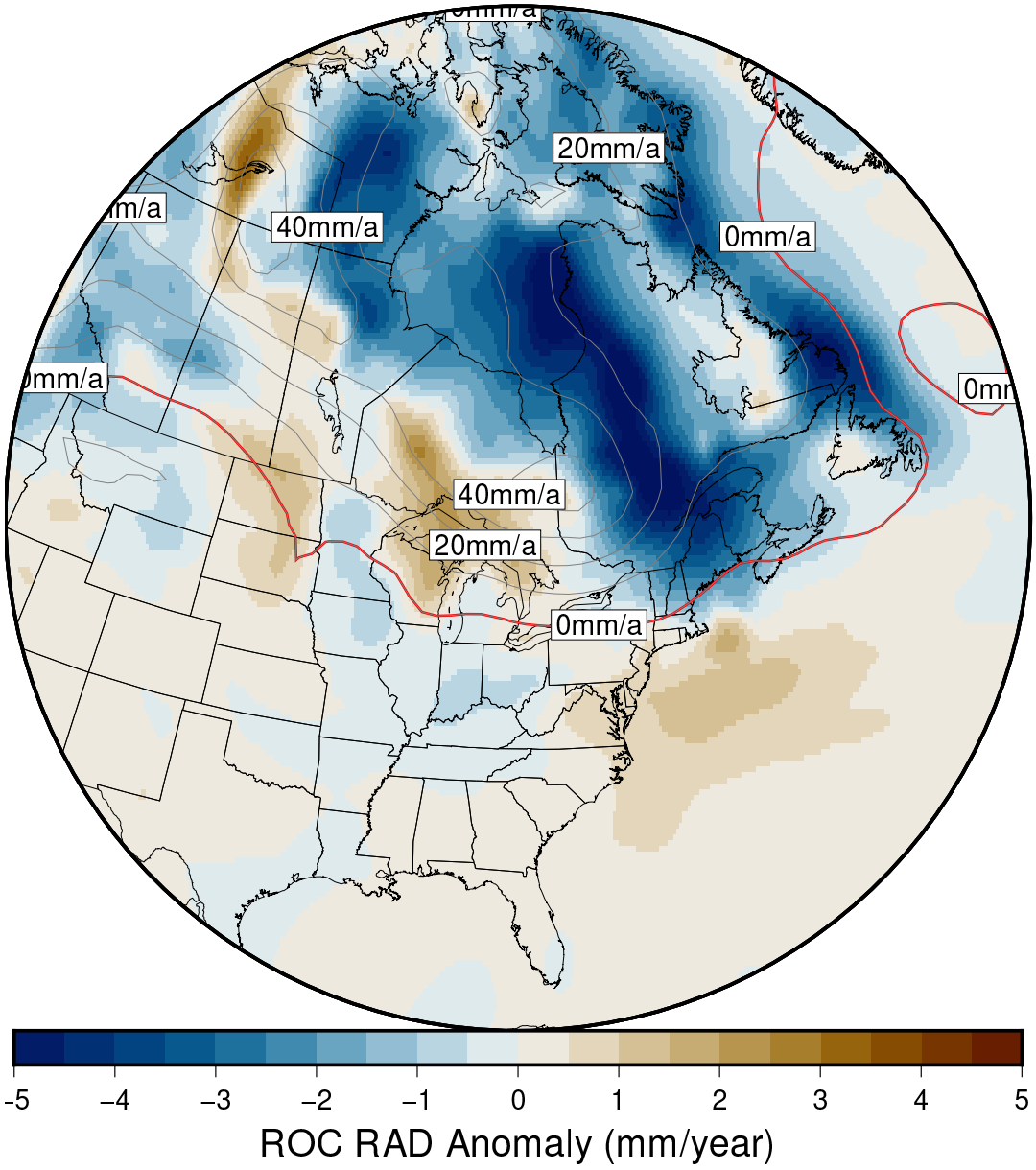

Figure S5. ROC RAD anomaly, emulated field minus 3D-SS field added to the NMSS output for the S40RTS+LR18 case, at 10ka. Contours denote the ROC RAD field (from from 3D-SS+NMSS) in 10 mm/yr increments, the red line denotes the 0 mm/yr contour. The parameter vector plotted is that with the median MSE, calculated for all spatio-temporal data, for the N = 45 ANN.

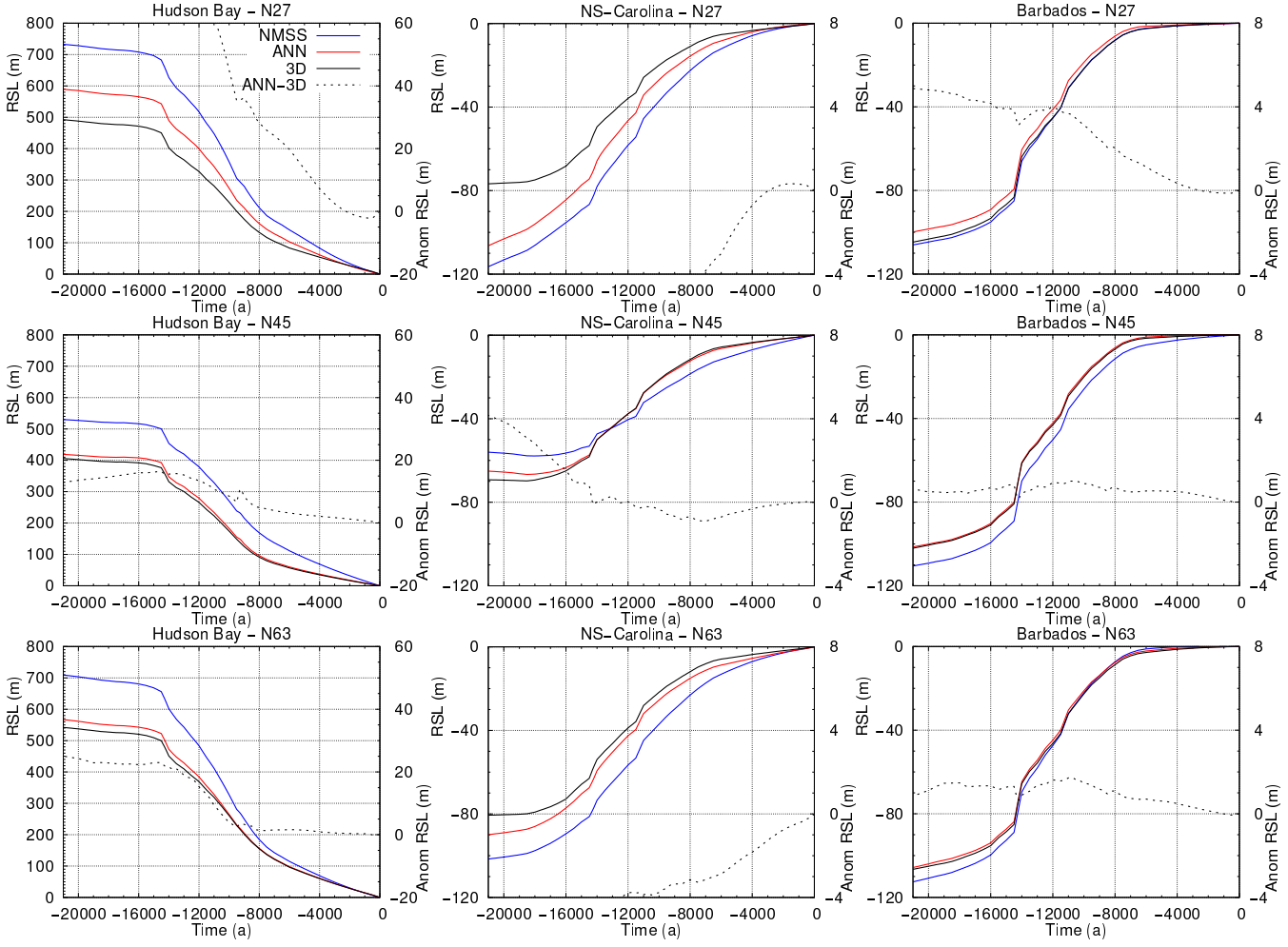

Figure S6. RSL timeseries for a near/ice-covered (Hudson Bay), intermediate (Northern S-Carolina), and far-field (Barbados) locations, for three of the trained ANNs which feature a reduced set of training ensemble members (number of parameter vectors included are denoted by N). Parameter vectors shown are drawn from the validation ensemble and are the median members (when considering the full spatio-temporal mean square error of the ANN). 3D Earth model configuration shown is the S40RTS with a SS lithosphere.

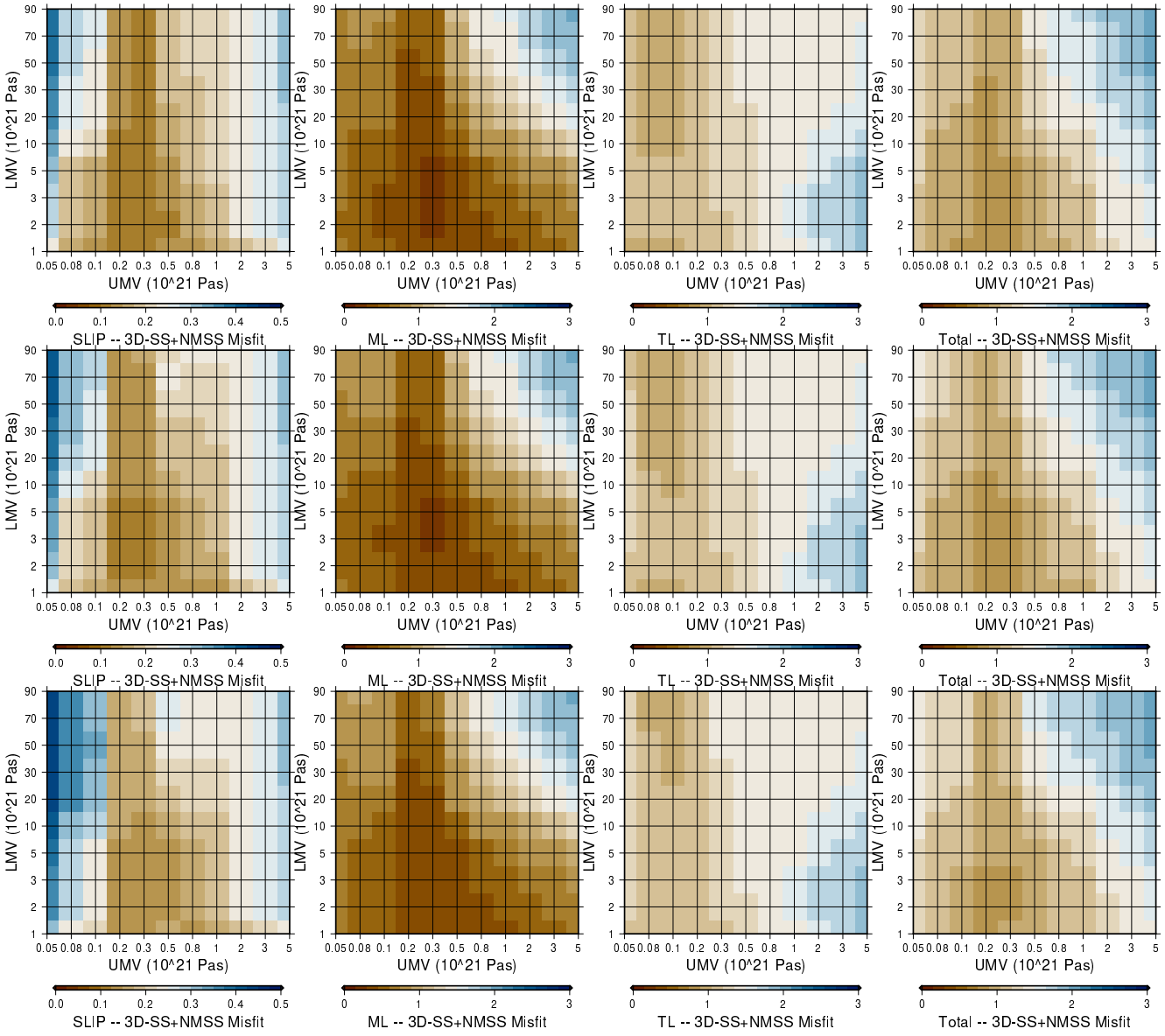

Figure S7. Misfit over parameter vectors for combined RSL database using explicit 3D model output (NMSS plus 3D-SS from Seakon) for S40RTS+LR18. Rows are different lithosphere thicknesses (71, 96, and 120km from top to bottom respectively).

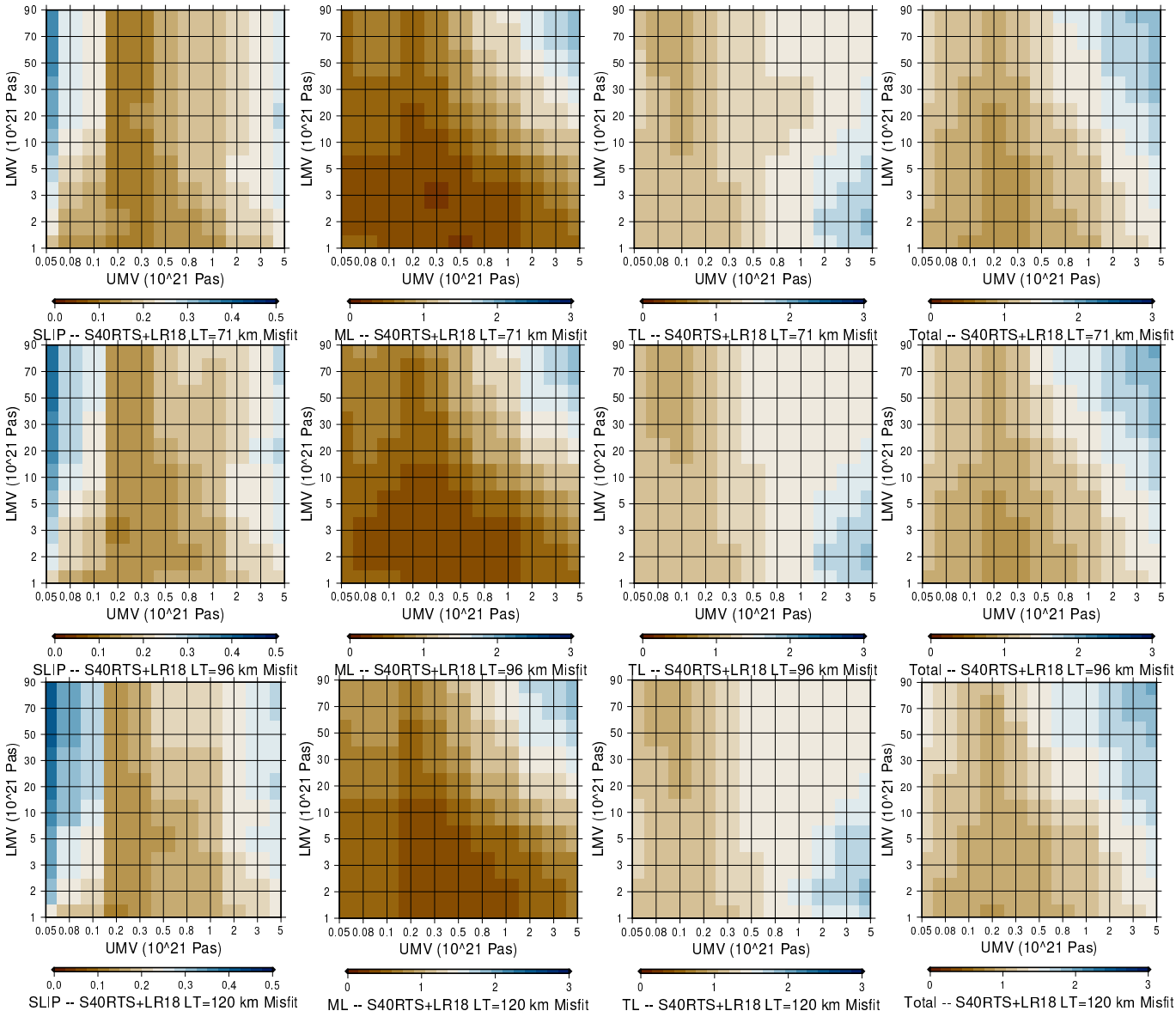

Figure S8. Plot shows misfit for the combined RSL database through parameter space (LT/UMV/LMV) for the NMSS model modified with the ANN to emulate S40RTS with the LR18 lithosphere model 3D Earth model. Columns from left to right show marine limiting, SLIP, terrestrial limiting, and total misfits respectively, while rows are 71, 96, and 120 km respectively. Misfit plotted is calculated as in equations 1 and 2.

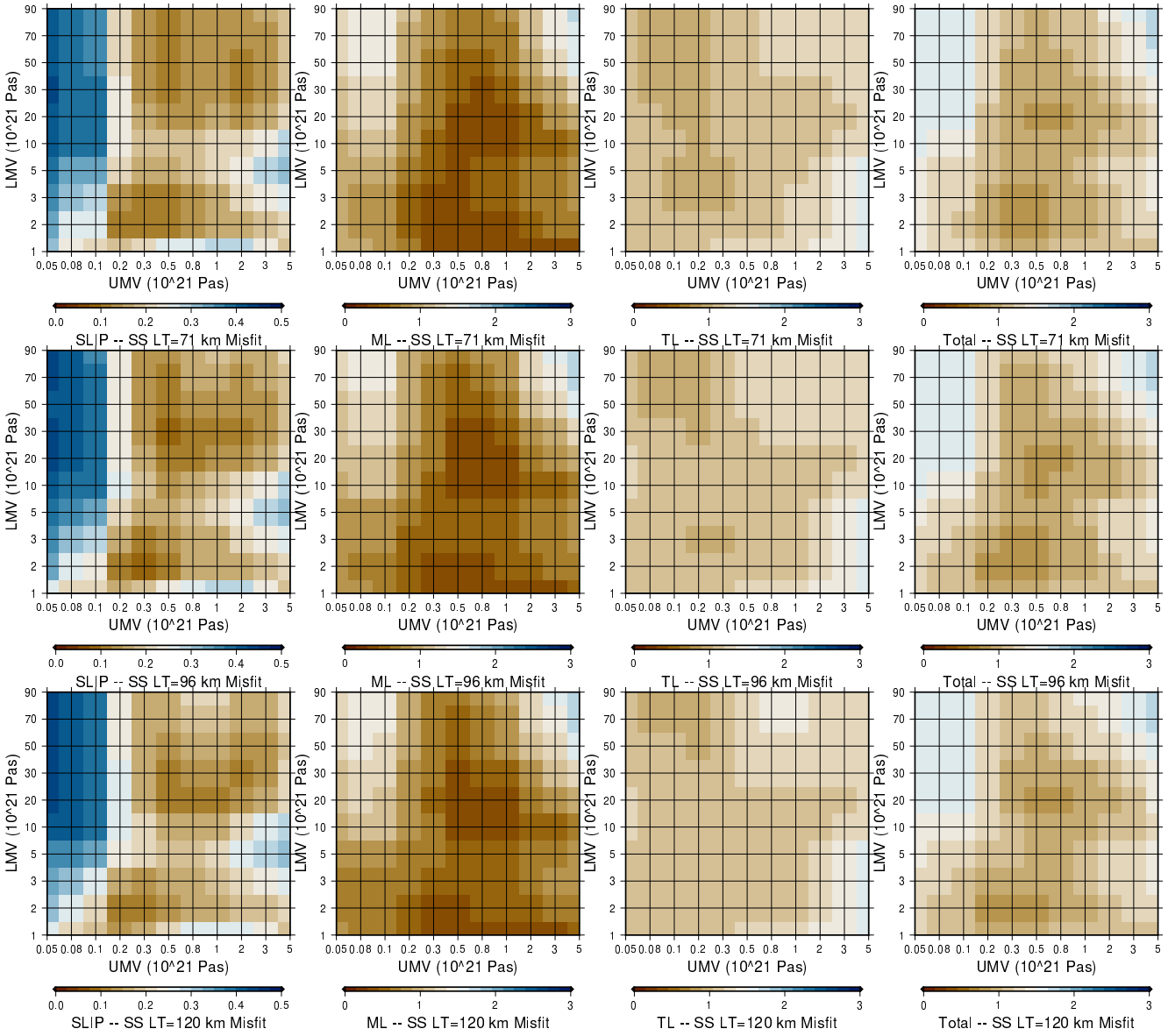

Figure S9. Plot shows misfit for the combined RSL database through parameter space (LT/UMV/LMV) for the NMSS model. Columns from left to right show marine limiting, SLIP, terrestrial limiting, and total misfits respectively, while rows are 71, 96, and 120 km respectively. Misfit plotted is calculated as in equations 1 and 2.

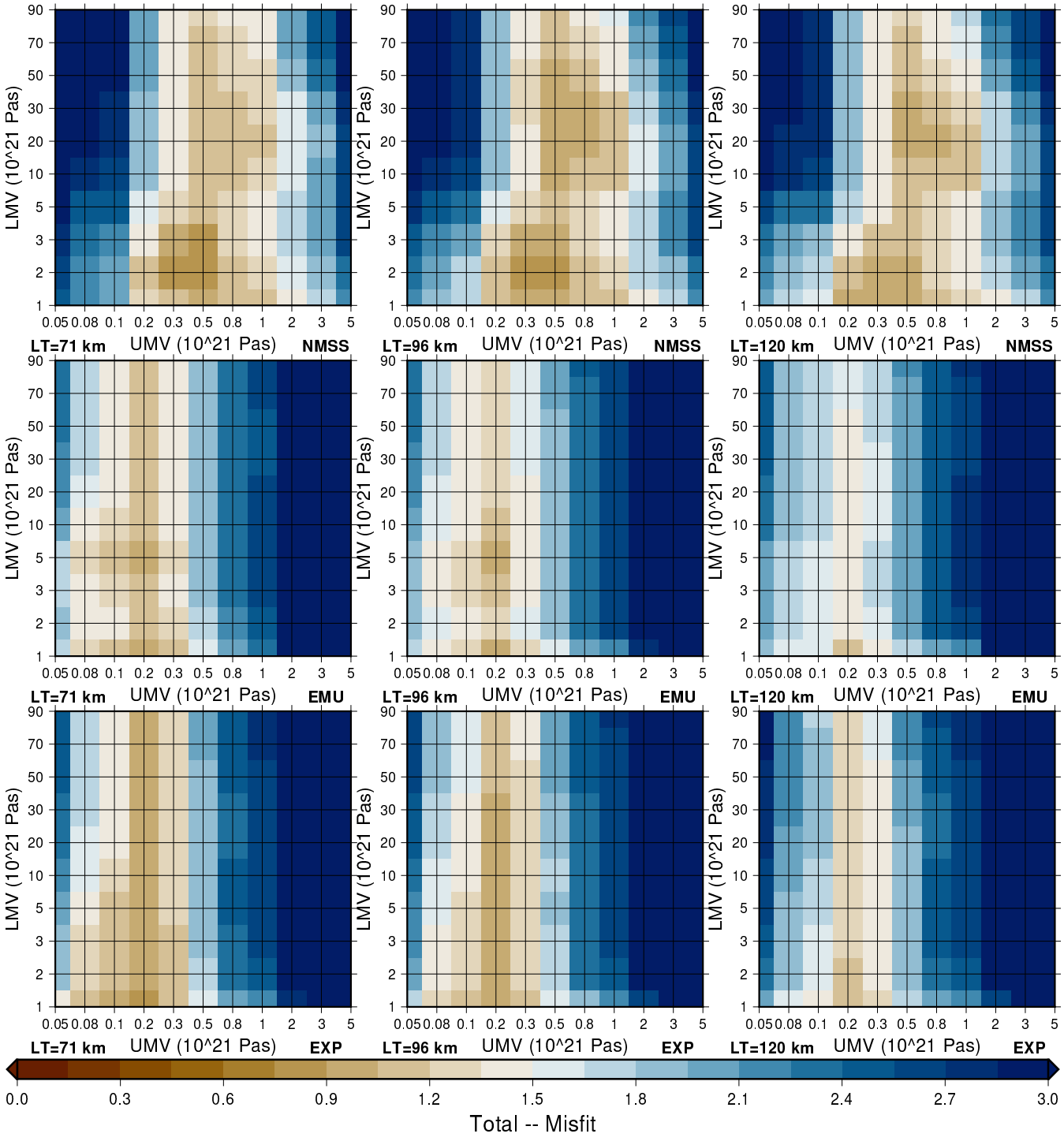

Figure S10. Model:data misfit across the CAAC RSL database through parameter space (LT/UMV/LMV). Top row is NMSS model output, middle row is emulated 3D model output (NMSS plus emulated 3D-SS from Seakon), bottom row is explicit (NMSS plus 3D-SS from Seakon) output. Misfit plotted is calculated as in equations 1 and 2 and total misfit has been plotted.

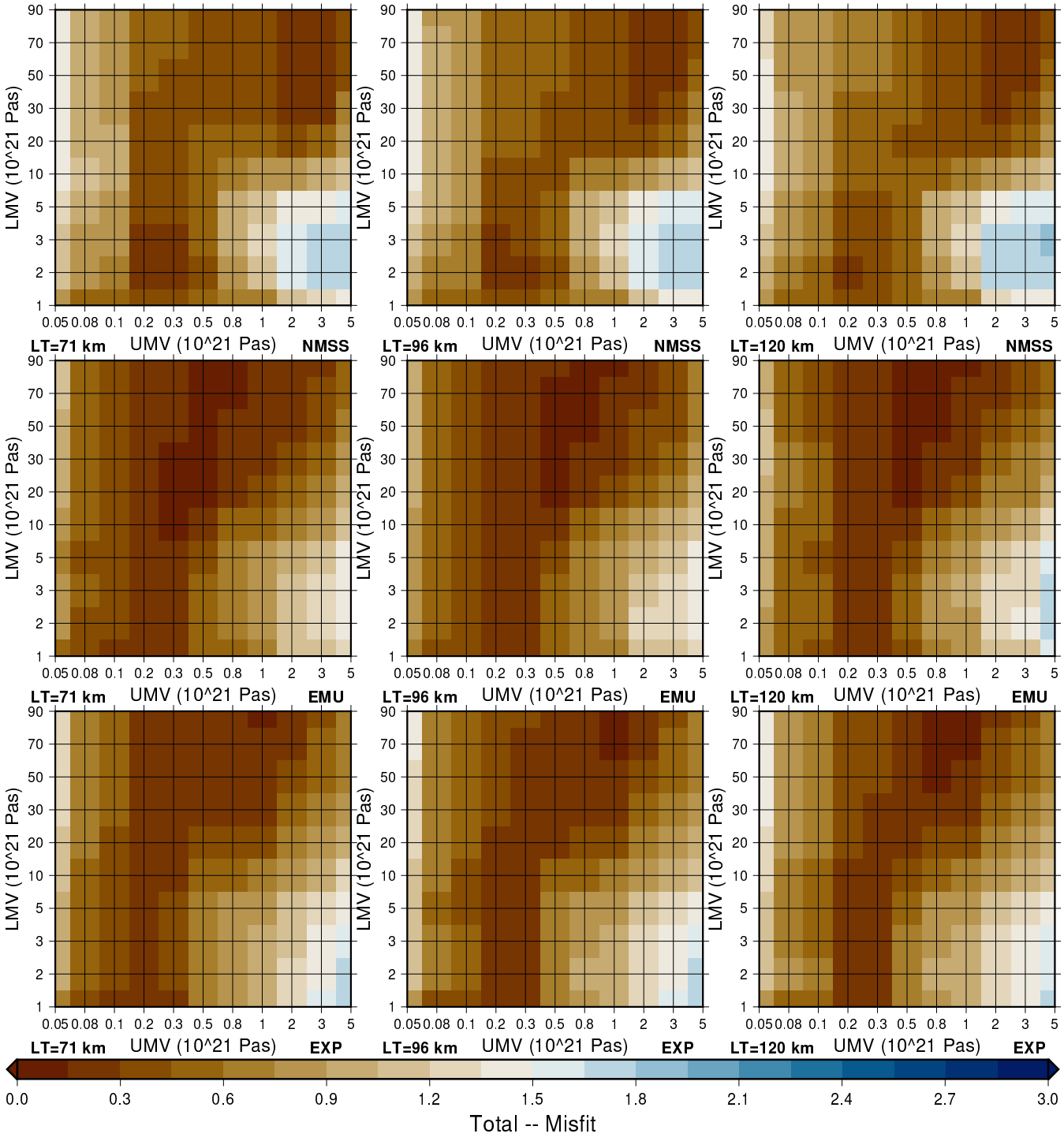

Figure S11. Model:data misfit across the USEC RSL database through parameter space (LT/UMV/LMV). Top row is NMSS model output, middle row is emulated 3D model output (NMSS plus emulated 3D-SS from Seakon), bottom row is explicit (NMSS plus 3D-SS from Seakon) output. Misfit plotted is calculated as in equations 1 and 2 and total misfit has been plotted.

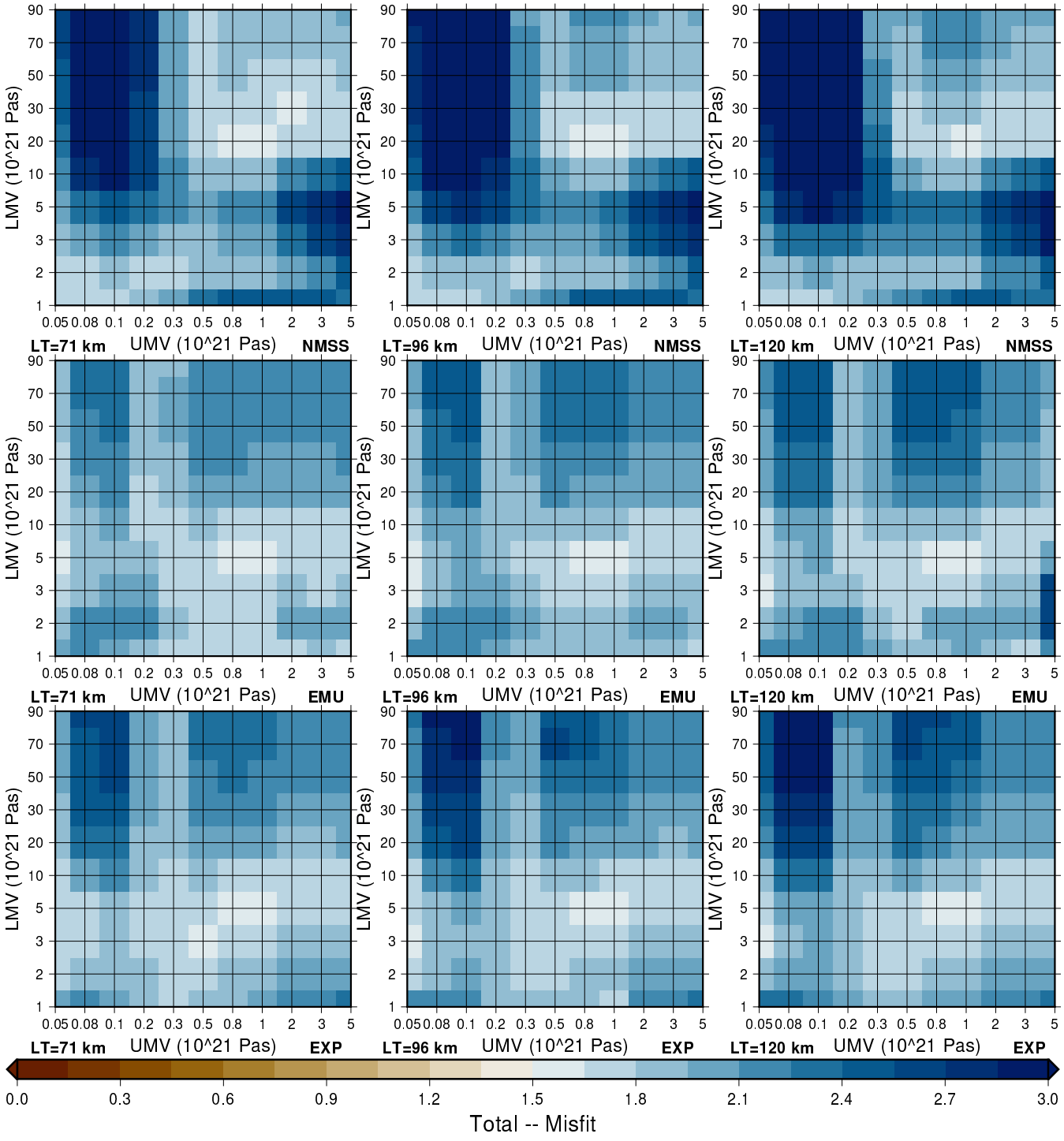

Figure S12. Model:data misfit across the USGC RSL database through parameter space (LT/UMV/LMV). Top row is NMSS model output, middle row is emulated 3D model output (NMSS plus emulated 3D-SS from Seakon), bottom row is explicit (NMSS plus 3D-SS from Seakon) output. Misfit plotted is calculated as in equations 1 and 2 and total misfit has been plotted.

References

Engelhart, S. E. and Horton, B. P.: Holocene sea level database for the Atlantic coast of the United States, Quaternary Science Reviews, 54, 12–25, https://doi.org/10.1016/j.quascirev.2011.09.013, 2012.

Love, R., Milne, G. A., Tarasov, L., Engelhart, S. E., Hijma, M. P., Latychev, K., Horton, B. P., and Törnqvist, T. E.: The contribution of glacial isostatic adjustment to projections of sea-level change along the Atlantic and Gulf coasts of North America, Earth's Future, 4, 440–464, https://doi.org/10.1002/2016ef000363, 2016.

Peltier, W.: GLOBAL GLACIAL ISOSTASY AND THE SURFACE OF THE ICE-AGE EARTH: The ICE-5G (VM2) Model and GRACE, Annual Review of Earth and Planetary Sciences, 32, 111–149, https://doi.org/10.1146/annurev.earth.32.082503.144359, 2004.

Vacchi, M., Engelhart, S. E., Nikitina, D., et al.: Postglacial relative sea-level histories along the eastern Canadian coastline, QSR, 201, 124–146, https://doi.org/10.1016/j.quascirev.2018.09.043, 2018.